

Dynamic mathematical model of the crystallization kinetics of fats

Imogen Foubert^{a,*}, Peter A. Vanrolleghem^b, Bert Vanhoutte^a, Koen Dewettinck^a

^a*Department of Food Technology and Nutrition, Faculty of Agricultural and Applied Biological Sciences, Ghent University, Coupure links 653, B-9000 Ghent, Belgium*

^b*Department of Applied Mathematics, Biometrics and Process Control—BIOMATH, Faculty of Agricultural and Applied Biological Sciences, Ghent University, Coupure links 653, B-9000 Ghent, Belgium*

Received 18 July 2002; accepted 16 August 2002

Abstract

A new model able to describe the kinetics of isothermal crystallization is presented: it is a model written in the form of a differential equation allowing use under dynamic temperature variations. It describes the crystallization process as if it is a reversible reaction with a first order forward reaction and a reverse reaction of order n . The model has the advantage of having an analytical solution under isothermal conditions that facilitates parameter estimation. The quality of this model was compared with the more traditional Avrami (with and without induction time) and Gompertz models using different model selection criteria. To show the universality of the model, different fat samples, different crystallization temperatures and different measuring techniques were used for model evaluation. The new model was selected as the best for the majority of the samples and this independent of the model selection criterion used.

© 2002 Elsevier Science Ltd. All rights reserved.

Keywords: Crystallization kinetics; DSC; Dynamic mathematical modeling; Fats; Isothermal crystallization; Lipids; Model selection; Parameter estimation

Fats are being crystallized for various reasons, such as fractionation into certain groups of triglycerides with varying melting and physical properties or to give food products a certain texture. Products in which fat crystallization is important include chocolates and confectionary coatings, dairy products such as butter and cream and vegetable spreads (margarine) (Hartel, 1992).

The crystallization process consists of two steps: nucleation and crystal growth. However, before any crystallization can take place, supersaturation or supercooling of the mother phase must be achieved (Boistelle, 1988). Nucleation can be described as a process in which molecules come into contact, orient and interact to form highly ordered structures, called nuclei. Crystal growth is the enlargement of these nuclei (Nawar, 1996). According to their environment, the crystals grow more or less regularly and exhibit different growth morphologies. Nucleation and crystal growth are not mutually exclusive: nucleation may take place while crystals grow

on existing nuclei. This makes it difficult to determine kinetics for each process separately (Boistelle, 1988).

The kinetics of fat crystallization, being dependent on the composition and on the processing conditions, is important for controlling operations in the food industry to produce the desired product characteristics (Metin & Hartel, 1998).

Thermal analysis methods such as differential scanning calorimetry (DSC) can be used to investigate the reaction kinetics of a broad range of materials, including metals, polymers and glass-forming solids. The two basic approaches to determine reaction kinetics are isothermal and non-isothermal methods. In isothermal experiments, such as used in this study, the sample is quickly brought to a predetermined temperature where the thermal analysis instrument monitors the behavior of the system as a function of time (Hatakeyama & Quinn, 1997). DSC has been used in the past to study the isothermal crystallization kinetics of natural fats (Kawamura, 1979; Metin & Hartel, 1998; Toro-Vazquez, Briceno-Montelongo, Dibildox-Alvarado, Charo-Alonso, & Reyes-Hernandez, 2000; and Ziegler, 1990). Other techniques commonly used to monitor fat

* Corresponding author. Tel.: +32-9-264-61-63; fax: +32-9-264-62-18.

E-mail address: imogen.foubert@rug.ac.be (I. Foubert).

crystallization are pulsed nuclear magnetic resonance (pNMR) and light-scattering techniques (Wright, Narine, & Marangoni, 2000). Authors that have used these techniques include Herrera, de Leon Gatti, and Hartel (1999), Kloek, Walstra, and van Vliet (2000) and Wright, Hartel, Narine, and Marangoni (2000).

The most generally used approach for the description of the isothermal phase transformation kinetics is the Avrami model developed in the 1940s. This equation is given as (Avrami, 1940):

$$f(t) = a^* (1 - e^{-k^* t^n}) \quad (1)$$

where f is the amount of solid fat at time t [%], a is the value for f as t approaches infinity [%], k is a crystallization rate constant which depends primarily on crystallization temperature [h^{-n}] and n is the Avrami exponent [], which is a combined function of the time dependence of nucleation and the number of dimensions in which growth takes place (Sharples, 1966). When using DSC to follow the crystallization kinetics, f is the released crystallization heat [J/g] and a is the latent heat [J/g]. Several researchers have used the Avrami model in the study of fat crystallization (Kawamura, 1979; Metin & Hartel, 1998; Toro-Vazquez et al., 2000; Wright, Hartel et al., 2000; Ziegleder, 1990).

Sometimes a fourth parameter is added to the Avrami model to account for an induction time t_i . The equation then becomes:

$$f(t) = a^* (1 - e^{-k^* (t-t_i)^n}) \quad (2)$$

Recently Kloek et al. (2000) used a modified Gompertz equation to describe the crystallization kinetics of fully hydrogenated palm oil in sunflower oil solutions. The Gompertz equation is often used to describe bacterial growth. There are indeed several analogies between fat crystallization and bacterial growth: the production of bacteria can be compared with the nucleation and growth of crystals, while the bacterial consumption of nutrients can be compared with the decrease of supersaturation. The reparameterized Gompertz equation is given by Zwietering, Jongenburger, Rombauts, and Van't Riet (1990):

$$f(t) = a^* \exp\left(-\exp\left(\frac{\mu^* e^*}{a} (\lambda - t) + 1\right)\right) \quad (3)$$

where f is the amount of solid fat at time t [%], a is the value for f as t approaches infinity [%], μ is the maximum increase rate in crystallization [%/h] (or the tangent to the inflection point of the crystallization curve) and λ is a measure for the induction time [h] defined as the intercept of the tangent at the inflection point with the time-axis.

It is the aim of this paper to present a new model able to better describe the isothermal crystallization kinetics

of fats. It is a dynamic model, having the advantage that it is easier to adapt for non-isothermal conditions. The model is fitted to isothermal crystallization data of some completely different fats, measured at different isothermal crystallization temperatures and using different measuring techniques (DSC and pNMR). The quality of the proposed model will be compared to the quality of the Avrami (with and without induction time) and Gompertz models.

1. Materials and methods

1.1. Materials

Fourteen different samples of cocoa butter (CB A–N) originating from Africa, South America as well as Asia, were crystallized isothermally (procedure, see Section 1.2) at 20 °C (CB .. /20). Each sample was analyzed in threefold. To check the influence of crystallization temperature on the quality of the three models, one cocoa butter (CB N) was crystallized isothermally at 19, 21, 22 and 23 °C (CB N/..). To check the influence of the type of fat on the quality of the four models, milk fat was crystallized isothermally at two different temperatures. Also, two samples of milk fat containing extra minor components were analyzed. To check the influence of measuring technique on the quality of the models, pNMR was, besides DSC, also used to record the isothermal crystallization kinetics of three milk fat fraction samples (procedure, see Section 1.4). Table 1 provides an overview of the samples and crystallization temperatures used.

1.2. DSC

The isothermal crystallization experiments were performed on a 2010 CE DSC (Texas Instruments, New Castle, DE, USA) with a Refrigerated Cooling System (Texas Instruments, New Castle, DE, USA). The DSC was calibrated with indium (TA Instruments, New Castle, DE, USA), azobenzene (Sigma-Aldrich, Bornem, Belgium) and undecane (Acros Organics, Geel, Belgium) prior to analyses. Nitrogen was used to purge the thermal analysis system. Fat (7.3–15.6 mg) was sealed into hermetic aluminum pans and an empty pan was used as a reference. The following temperature protocol was used for the isothermal crystallization experiments of cocoa butter (Foubert, Vanrolleghem, & Dewettinck, accepted for publication): hold at 65 °C for 15 min to ensure a completely liquid state, cool at 8 °C/min to the isothermal crystallization temperature and hold at that temperature until crystallization has finished. For the isothermal crystallization experiments of milk fat the initial melting step was changed to 70 °C for 5 min, the rest of the temperature protocol being the same as for

cocoa butter. The changes in the heat flow during isothermal DSC operation at crystallization temperature were recorded.

1.3. DSC crystallization curves

The amount of heat released as a function of time was calculated by integration of the isothermal crystallization curves using a horizontal sigmoid baseline. The start and end points of the crystallization curve were determined using an objective calculation algorithm (Foubert et al., 2002). Summarized, this algorithm works as follows: the slope of the heat flow is calculated, the time at which the slope changes from a negative to a positive slope before the peak maximum is taken as the start point and the time at which the slope changes sign for the third time after the peak maximum is taken as the end point. In between start and end points the area (and thus the amount of heat released up to that moment) was calculated. The integration was performed using the Universal Analysis software version 2.5 H (Texas Instruments, New Castle, DE, USA).

1.4. pNMR

pNMR measurements were performed with a Minispec pc 20 (Bruker, Karlsruhe, Germany). Samples were heated at 60 °C for 1 h before analysis to eliminate any thermal history. The samples were then placed in a thermostated water bath and readings were taken at appropriate time intervals.

1.5. Parameter estimation

The data series were fitted to the different algebraic models by non-linear regression using the Sigmaplot 2000 software (SPSS Inc., Chicago, IL, USA). This software uses the Marquardt–Levenberg algorithm to find the parameters that give the ‘best fit’ between the model and the data. This algorithm seeks the values of the parameters that minimize the sum of squared differences between the observed and predicted values of the dependent variable. The process is iterative: the curve fitter begins with a guess at the parameters, checks to see how well the model fits and then continues to make better guesses until the differences between the residual sum of squares no longer decreases significantly. This condition is known as convergence. By varying the initial values, step size and tolerance, it is avoided that the iterative process stops in a local minimum.

The parameter estimations of the model in its differential equation form were performed in WEST (Hemmis NV, Kortrijk, Belgium, <http://www.hemmis.be>) using the Simplex algorithm (Nelder & Mead, 1965).

1.6. Model selection

Several methods exist to evaluate the quality of different models after fitting each model to the data. These methods can be subdivided in information criteria, methods that go back to statistics and techniques in which an analysis is made of the residuals between model predictions and measured data. Vanrolleghem

Table 1
Overview of used samples

| Sample name | Sample description | Crystallization temperature (°C) |
|-------------|--|----------------------------------|
| CB A | Cocoa butter from West-Africa (ADM Cocoa, Koog aan de Zaan, Netherlands) | 20±0.05 |
| CB B | Cocoa butter from Ivory Coast (1 st sample) (Barry Callebaut, Wieze, Belgium) | 20±0.05 |
| CB C | Cocoa butter from Nigeria (Barry Callebaut, Wieze, Belgium) | 20±0.05 |
| CB D | Cocoa butter from Ivory Coast (2 nd sample) (Barry Callebaut, Wieze, Belgium) | 20±0.05 |
| CB E | Cocoa butter from Indonesia (Barry Callebaut, Wieze, Belgium) | 20±0.05 |
| CB F | Cocoa butter from Malaysia (ADM Cocoa, Koog aan de Zaan, Netherlands) | 20±0.05 |
| CB G | Cocoa butter from San Domingo (Barry Callebaut, Wieze, Belgium) | 20±0.05 |
| CB H | Cocoa butter from Ecuador (Barry Callebaut, Wieze, Belgium) | 20±0.05 |
| CB I | Cocoa butter from Brazil (Barry Callebaut, Wieze, Belgium) | 20±0.05 |
| CB J | Unsteamed cocoa butter (unknown origin) (Bensdorp, Barry Callebaut, Bussum, Netherlands) | 20±0.05 |
| CB K | Steamed cocoa butter (unknown origin) (Bensdorp, Barry Callebaut, Bussum, Netherlands) | 20±0.05 |
| CB L | Cocoa butter (unknown origin) (Barry Callebaut, Wieze, Belgium) | 20±0.05 |
| CB M | Hard cocoa butter (unknown origin) (Barry Callebaut, Wieze, Belgium) | 20±0.05 |
| CB N | Standard factory product cocoa butter (Barry Callebaut, Wieze, Belgium) | 19,20,21,22,23±0.05 |
| MF A | Milk fat (Aveve Dairy Products, Klerken, Belgium) | 20.7±0.05 23.7±0.05 |
| MF B | Purified milk fat (Aveve Dairy Products, Klerken, Belgium)+0.5% water | 23.7±0.05 |
| MF C | Purified milk fat (Aveve Dairy Products, Klerken, Belgium)+0.75% water +0.075% phospholipids | 23.7±0.05 |
| MF D | Milk fat fraction 1 (Aveve Dairy Products, Klerken, Belgium) | 17.5 °C |
| MF E | Milk fat fraction 2 (Aveve Dairy Products, Klerken, Belgium) | 21.5 °C |
| MF F | Milk fat fraction 3 (Aveve Dairy Products, Klerken, Belgium) | 26 °C |

and Dochain (1998) give an overview of the model selection methods. The methods used in this study are summarized below.

The two best-known information criteria are the Final Prediction Error (FPE) and Akaike's Information Criterion (AIC):

$$\text{FPE} = \frac{\text{SSR}}{N} * \left(1 + \frac{2 * p}{N - p}\right) \quad (4)$$

$$\text{AIC} = N * \log\left(\frac{\text{SSR}}{N}\right) + 2 * p \quad (5)$$

where SSR is the sum of squared residuals, p is the number of parameters in the model and N is the number of data points. The model with the smallest criterion value is in each case selected. These criteria have the disadvantage that they are not consistent (i.e. do not guarantee that the probability of selecting the wrong model tends to zero as the number of data points tends to infinity). Examples of consistent criteria are the Bayesian Information Criterion (BIC) and LILC:

$$\text{BIC} = N * \log\left(\frac{\text{SSR}}{N}\right) + p * \log(N) \quad (6)$$

$$\text{LILC} = N * \log\left(\frac{\text{SSR}}{N}\right) + p * \log(\log(N)) \quad (7)$$

The model with the lowest criterion value is selected

The statistical F -test is probably the most frequently applied method to decide whether the more complex model j is significantly (with a confidence level α) better than model i . The calculated value

$$F_w = \frac{(\text{SSR}_i - \text{SSR}_j) / (p_j - p_i)}{\text{SSR}_j / (N - p_j)} \quad (8)$$

has to be compared with tabulated values for $F_{\alpha}(p_j - p_i, N - p_j)$.

The quality of a model can also be assessed by analysis of the properties of the calculated residuals ε (measured value – predicted value). Two approaches can be used to check whether the residuals are independent of each other. The so-called run test evaluates the number of sign changes in the residual sequence and compares that to the expected number $N/2$. The autocorrelation test consists of comparing the value of the autocorrelation r for each lag τ with the limit value $N(0, 1)/\sqrt{N}$ with $N(0, 1)$ the standard normal distribution. For a significance level $\alpha = 0.05$ this means that only 5% of the autocorrelations may be larger than $1.96/\sqrt{N}$. The autocorrelation with time lag τ quantifies the dependency of a variable at any time t_k and the variable at time $(t_k - \tau)$:

$$r(\tau) = \frac{1}{r(\tau = 0)} * \sum_{k=1}^{N-\tau} \varepsilon(t_k - \tau) * \varepsilon(t_k) \quad (9)$$

The value for the autocorrelation test is the amount of autocorrelations being higher than the threshold value.

The Sigmaplot software provided an additional criterion that was used in this study. It is the predicted residual error sum of squares (PRESS) that gauges how well a regression model predicts new data. The smaller the PRESS statistic, the better the predictive ability of the model. The PRESS statistic is computed by summing the squares of the prediction errors (differences between predicted and observed values) for each observation, with that point deleted from the computation of the regression equation.

2. Results and discussion

2.1. The model

A new model, able to describe the isothermal crystallization kinetics of fats, was developed. The model was, in contrast to the Avrami and Gompertz models, written in the form of a differential equation. This type of equation has the advantage that (i) it is often easier to interpret the equation mechanistically, (ii) it is easier to make minor changes to the equation on the basis of acquired knowledge and (iii) by incorporation of secondary models describing the temperature dependency of the parameters, the model can be used to describe non-isothermal crystallization kinetics. In contrast, an algebraic solution is obtained assuming isothermal conditions, making its use for non-isothermal conditions impossible. An algebraic solution however, offers the advantage that parameter estimation is easier because of more readily available software packages capable of non-linear regression of algebraic equations. Therefore, both the differential equation and the algebraic solution of the simplified version are presented in this paper. When using the Avrami and Gompertz models the amount of solid fat f is expressed as a function of time. For ease of presentation however, the differential equation of this model is expressed in terms of a related variable h , which is the remaining crystallizable fat:

$$h = \frac{a - f}{a} \quad (10)$$

where a is the value of the variable f for t approaching infinity. In contrast to f , which increases with time in a sigmoidal way, this new variable h is related to the remaining supersaturation (i.e. the driving force of crystallization) and thus decreases in a sigmoidal way with time.

To build the model, the approach of Wunderlich (1990) was followed. He states that phase transitions (such as crystallization) can be written in the form of a chemical reaction:

A (in this case melt) \rightleftharpoons B (in this case crystals)

and that for the thermodynamic and kinetic description of phase transitions the same equations as for chemical reactions can be used. Furthermore, he states that all transitions between the molten and the crystalline phase are usually assumed to be first-order transitions. Common causes, however, for a deviation of a first order transition are impurities and a distribution of phases with different perfections.

In this work, the crystallization process is represented as if it was a combination of a first-order forward reaction and a reverse reaction of order n with rate constants K_i for each of the chemical reactions. The dynamics of h can then mathematically be written as:

$$\frac{dh}{dt} = K_n^* h^n - K_1^* h \quad (11)$$

K_1 and K_n are the rate constants of the first order forward reaction and the n th order reverse reaction, respectively.

The detailed nature of the reverse reaction is yet unknown, but it might be related to re-melting of some crystals due to dissipation of latent heat of crystallization.

To calculate the values of h as a function of time according to Eq. (11), the initial value for h , $h(0)$, needs to be specified:

$$h(0) = \frac{a - f(0)}{a} \quad (12)$$

$f(0)$ is then the initially present amount of crystals (nuclei?). The background of this variable is difficult to explain mechanistically but it will be shown further that $f(0)$ can be related to the induction time of the crystallization process. The parameters of this model therefore are $f(0)$, n , K_n , K_1 and a .

Extensive parameter estimation studies revealed a difference between K_1 and K_n of only around 1.10^{-5} (results not shown). Furthermore, the quality of the five-parameter model was found not to be significantly better than that of a four-parameter model for which $K_1 = K_n$. It was thus decided to simplify the model to:

$$\frac{dh}{dt} = K^*(h^n - h) \quad h(0) = \frac{a - f(0)}{a} \quad (13)$$

in which a is the value of f when t approaches infinity [expressed in percent (solid fat potential) when measuring

by means of pNMR, expressed in J/g (latent heat) when measuring by means of DSC], K is the rate constant (expressed in h^{-1}), n is the order of the reverse reaction (dimensionless) and $f(0)$ is the initially present amount of crystals (expressed in J/g when measuring by means of DSC).

The behavior of the generalized form of Eq. (11), with n_2 as the order of the forward reaction instead of a fixed value of one, was also explored. Parameter estimation studies revealed that the fit of this generalized equation was not significantly better than that of Eq. (11). Typical values obtained for n_2 were 0.88, 0.89 and 0.92.

Fig. 1 shows the influence of the four parameters on the crystallization curve. Fig. 1A shows the influence of varying a between 40 and 70 J/g [$f(0) = 1.10^{-5}$ J/g, $K = 6 h^{-1}$, $n = 5$]. The parameter a is indeed the height of the plateau and thus directly related to the a values of the Avrami and Gompertz models.

Fig. 1B shows the influence of varying $f(0)$ between 1.10^{-7} and 1.10^{-4} J/g ($a = 60$ J/g, $K = 6 h^{-1}$, $n = 5$). The parameter $f(0)$ is clearly related to the induction time of the crystallization process. To make this relationship clearer $f(0)$ was mathematically related to the induction time $t_{ind,x}$ which is defined here as the time needed to reach $x\%$ of crystallization, where x could for example be 1%:

$$t_{ind,x} = \frac{-\ln\left(\frac{(1-x)^{1-n}-1}{\left(1-\frac{f(0)}{a}\right)^{1-n}-1}\right)}{(1-n)^*K} \quad (14)$$

Fig. 1C shows the influence of varying K between 3 and $12 h^{-1}$ [$a = 60$ J/g, $f(0) = 1.10^{-5}$ J/g, $n = 5$]. The rate of crystallization obviously increases when the K parameter increases. Thus, the higher the value of K , the shorter the time needed to reach a measurable amount of solid fat and the faster the rest of the crystallization process takes place. In the case of $K = 3$ the crystallization rate is so slow that the plateau (60 J/g) is not yet reached after 2.5 h.

Fig. 1D shows the influence of varying n between 1.5 and 7 [$a = 60$ J/g, $K = 10 h^{-1}$, $f(0) = 1.10^{-5}$ J/g]. The parameter n also has an influence on the time needed to reach a measurable amount of solid fat. This can be explained as follows: the higher the n value (i.e. the order of the reverse reaction), the faster the term $K * h^n$ will become negligible and the faster a relevant amount of solid fat will be formed. However, the value of n is also linked with the degree of curve asymmetry. When the value of n is 2, the sigmoidal curve is perfectly symmetric. When the value is larger than 2, the beginning of the crystallization process is faster than the end. The more n exceeds 2, the larger the difference between the rates of the beginning and end stages becomes. When

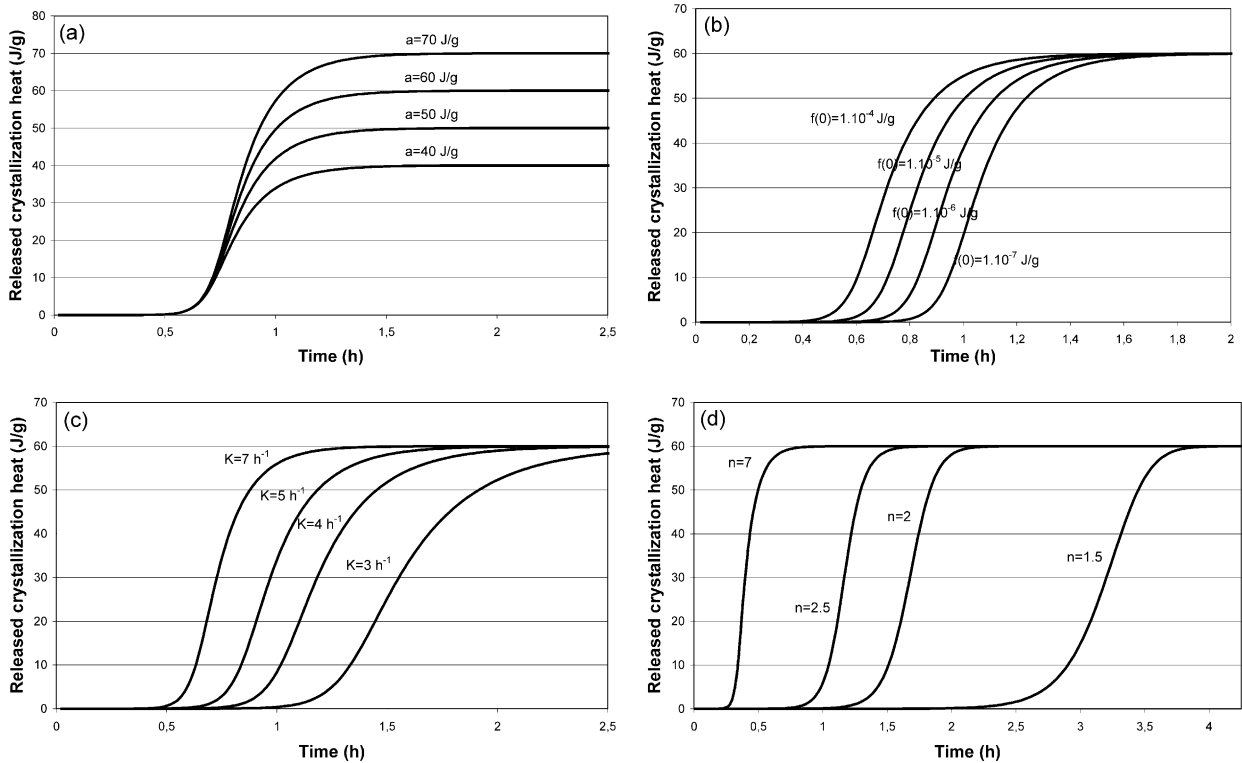


Fig. 1. (a) Influence of the parameter a on the crystallization curve [$f(0) = 1.10^{-5}$ J/g, $K = 6$ h $^{-1}$]. (b) Influence of the parameter $f(0)$ on the crystallization curve ($a = 60$ J/g, $K = 6$ h $^{-1}$). (c) Influence of the parameter K on the crystallization curve [$a = 60$ J/g, $f(0) = 1.10^{-5}$ J/g]. (d) Influence of the parameter n on the crystallization curve [$a = 60$ J/g, $f(0) = 1.10^{-5}$ J/g, $K = 10$ h $^{-1}$, $n = 5$].

the value is smaller than 2, the beginning of the process is slower than the end. This influence of n on the degree of curve asymmetry is illustrated in Fig. 2. In this figure the time-axis was normalized by rescaling time such that all curves intersect at 50% of their ultimate value.

Table 2 shows some typical parameter ranges obtained for the analyzed samples. The parameters obviously show a temperature and sample dependency.

2.2. Algebraic solution

To simplify parameter estimation the differential equation (four parameter model) was converted to its

algebraic solution. To solve the differential Eq. (13) it is rewritten as:

$$h^{-n} \frac{dh}{dt} + K^* h^{1-n} - K = 0 \tag{15}$$

When h^{1-n} is substituted by z , this leads to the first order differential equation:

$$\frac{1}{1-n} \frac{dz}{dt} + K^* z = K \tag{16}$$

The solution of which is

$$z = 1 + (z(0) - 1) * e^{-(1-n)*K^*t} \tag{17}$$

After re-substitution into the original variable h , this leads to

$$h = \left[1 + (h(0)^{1-n} - 1) * e^{-(1-n)*K^*t} \right]^{\frac{1}{1-n}} \tag{18}$$

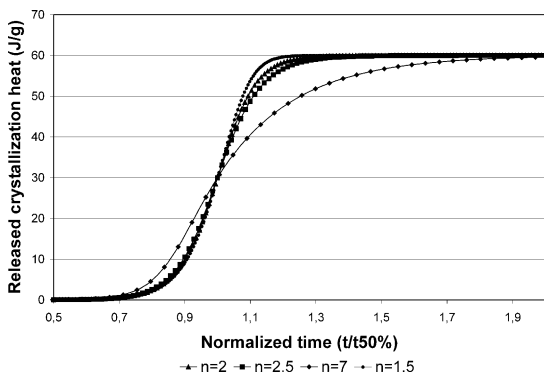


Fig. 2. Influence of the parameter n on the curve asymmetry [normalized time-axis, $a = 60$ J/g, $f(0) = 1.10^{-5}$ J/g, $K = 10$ h $^{-1}$, $n = 5$].

Table 2
Typical parameter ranges of the proposed model

| Sample | a (J/g) | K (h $^{-1}$) | n | $f(0)$ (J/g) |
|-----------------------|-----------|------------------|-------|---------------------------|
| Cocoa butter at 20 °C | 60–70 | 4–7 | 3–6 | 1.10^{-5} – 1.10^{-3} |
| Cocoa butter at 22 °C | 55–65 | 2.5–3.5 | 3.5–4 | 1.10^{-3} – 2.10^{-2} |
| Milk fat samples | 10–20 | 3–12 | 3–6 | 1.10^{-6} – 1.10^{-3} |

As mentioned before $h(0)$ is, via $f(0)$, related to the induction time of crystallization. Since the physical interpretation of the parameter induction time is more straightforward than that of the parameter $h(0)$ [or the equivalent $f(0)$] and since the induction time can be more easily found back on a crystallization curve it was decided to represent the equation as a function of t_{ind_x} instead of $h(0)$. Using Eq. (14), $h(0)$ can be expressed as a function of t_{ind_x} and this relationship can then be inserted into Eq. (18). After simplification this then leads to:

$$h = \left[1 + ((1 - x)^{1-n} - 1)^* e^{-(1-n)*K*(t-t_{\text{ind}_x})} \right]^{\frac{1}{1-n}} \quad (19)$$

where x is the percentage of fat in the definition of the induction time t_{ind_x} [Eq. (14)].

Eq. (19) can be used in many software packages capable of parameter estimation of non-linear algebraic equations.

In this work, preference was given to this algebraic solution for parameter estimation.

2.3. Model selection

For each sample, Table 3 shows the results of the model selection using the different model selection criteria. The four information criteria (FPE, AIC, BIC and LILC) and the PRESS criterion give the same result for most of the samples, i.e. the proposed model performs the best for most of the samples. For some samples the quality of fit of the Gompertz and the proposed model is so similar that on the basis of some criteria the Gompertz model is selected, while on the basis of other criteria the proposed model is selected. All information criteria are based on the sum of squared residuals and thus give an indication of how much the predicted curve differs from the actually measured curve, compensating in different ways for model complexity.

The statistical F -test shows that for all samples the proposed model performs significantly ($\alpha=0.01$ except for one sample, $\alpha=0.05$) better than the Avrami model without induction time and for most of the samples also significantly better than the Gompertz model. Comparison of the proposed model with the Avrami model with induction time is not possible using an F -test since both models contain the same number of parameters [see Eq. (8)]. On the basis of the information criteria discussed above, it could however be concluded that the proposed model performs better than the Avrami model with induction time for all samples studied.

To get a better insight in the magnitude of the difference between the Gompertz and the proposed model the values for the mean sum of squared residuals (MSR) ($= \text{SSR}/(N-p)$) for both models are presented in Table 4 for each sample. The MSR value consists of the

measurement error and the model error. Since the measurement error can be assumed constant, the model is better as the value of MSR is lower and the bigger the difference between the values for MSR, the bigger the difference between the quality of the models. From Table 4 it can be seen that the MSR value is much more constant for the proposed model than for the Gompertz model. For some samples the values for the Gompertz model are only slightly higher, or for some samples even slightly lower than for the proposed model while for other samples the MSR value for the Gompertz model is much higher than that for the proposed model. For the samples where the proposed model performs worse, the difference between the two values is small. These results indicate that the proposed model is more flexible in describing the crystallization kinetics of fats. It gives a good fit for all the samples used in this study, while the Gompertz model gives some very good fits, but also some significantly poorer fits.

When modeling, the residuals are assumed to be random and independent. As explained above, the run and autocorrelation tests give an idea of how good this assumption is satisfied. The value for the run test should, for the DSC measurements, be around 10 (knowing that the number of data points fluctuates around 20). The values obtained for each of the four models are between 3 and 6 for most samples. The model with the highest number of sign changes can be regarded as the best. Table 3 shows that for nearly all samples the proposed model is selected as (one of) the best.

The autocorrelation may only be larger than 0.44 (approximate value for $1.96/\sqrt{N}$) for 1 lag (i.e. 5% of the 18 lags that were calculated). For the proposed model a maximum of one autocorrelation is found above the threshold value for all samples considered. For the other models there are a limited number of samples for which more than one autocorrelation is above the threshold.

Next to mathematical tools, one can also assess the quality of a model visually. Fig. 3A–D show the measured data points together with the predicted curves calculated with the Avrami (with and without induction time), the Gompertz and the proposed model and the residuals for each of the models. Fig. 3A and C represent sample CB N/19, the sample for which the difference between the Gompertz and the proposed model is the biggest (in the advantage of the proposed model), while Fig. 3B and D represent sample CB D/20(3), the sample for which the difference between the two models is the biggest in the advantage of the Gompertz model. For both samples it can be seen that the Gompertz and the proposed model are much closer to the data than the Avrami model. For sample CB N/19 (Fig. 3A/C) the Avrami model with induction time seems to have a comparable quality of fit than the Gompertz model, a fit which is however considerably worse than that of the

Table 3

Model selected on the basis of different model selection criteria (A = Avrami, Ai = Avrami with induction time, G = Gompertz, F = Foubert)

| Sample | FPE | AIC | BIC | LILC | PRESS | Run test | Auto-correlation test | F-test ($\alpha=0.01$) |
|-------------------------------|--------------|--------------|--------------|--------------|--------------|--------------|-----------------------|--------------------------|
| CBA/20 (1) | F | F | F | F | F | F | A/Ai/F/G | F |
| CBA/20 (2) | F | F | F | F | F | F | A/Ai/F/G | F |
| CBA/20 (3) | F | F | F | F | F | F | F | F |
| CBB/20 (1) | F | F | F | F | F | G | A/Ai/F/G | F |
| CBB/20 (2) | F | F | F | F | F | F | A/Ai/F/G | F |
| CBB/20 (3) | F | F | F | F | F | F | A/Ai/F | F |
| CBC/20 (1) | F | F | F | F | F | F | F | F |
| CBC/20 (2) | F | F | F | F | F | F | Ai/F/G | F |
| CBC/20 (3) | F | F | F | F | F | F | F/G | F |
| CBD/20 (1) | F | F | F | F | F | F | A/Ai/F | F |
| CBD/20 (2) | F | F | F | F | F | F | A/Ai/F/G | F |
| CBD/20 (3) | G | G | G | G | G | G | F/G | G |
| CBE/20 (1) | G | G | G | G | G | F/G | A/Ai/F/G | G ^a |
| CBE/20 (2) | F | F | F | F | G | F | A/Ai/F/G | F |
| CBE/20 (3) | G | G | G | G | G | F | F | G |
| CBF/20 (1) | F | F | F | F | F | F | A/Ai/F/G | F |
| CBF/20 (2) | G | G | G | F | F | F | F/G | G |
| CBF/20 (3) | F | F | F | F | F | F | A/Ai/F/G | F |
| CBG/20 (1) | G | G | G | G | G | F | A/Ai/F/G | F/G |
| CBG/20 (2) | F | F | F | F | F | Ai/F | A/Ai/F/G | F |
| CBG/20 (3) | F | F | F | F | F | F | A/Ai/F/G | F |
| CBH/20 (1) | F | G | G | F | G | F | F/G | F/G |
| CBH/20 (2) | G | G | G | G | G | G | A/Ai/F/G | G |
| CBH/20 (3) | G | G | G | G | G | Ai/F | A/Ai/F/G | G ^a |
| CBI/20 (1) | F | F | F | F | F | F | A/Ai/F/G | F |
| CBI/20 (2) | F | F | F | F | F | F | A/Ai/F/G | F |
| CBI/20 (3) | F | F | F | F | F | F | F/G | F |
| CBJ/20 (1) | G | G | G | G | G | F | A/Ai/F/G | F/G |
| CBJ/20 (2) | F | F | F | F | F | F | A/Ai/F/G | F |
| CBJ/20 (3) | F | F | F | F | F | G | A/Ai/F/G | F ¹ |
| CBK/20 (1) | F | F | F | F | F | F | F | F |
| CBK/20 (2) | F | F | F | F | F | F | F | F |
| CBK/20 (3) | F | F | F | F | F | F | F | F |
| CBL/20 (1) | G | G | G | G | G | F | F | F/G |
| CBL/20 (2) | G | G | G | G | G | F | F | G |
| CBL/20 (3) | F | F | F | F | F | Ai/F | A/Ai/F/G | F |
| CBM/20 (1) | F | F | F | F | F | Ai/F | Ai/F/G | F |
| CBM/20 (2) | F | F | F | F | F | Ai/F/G | A/Ai/F/G | F |
| CBM/20 (3) | F | F | F | F | F | F | F | F |
| CBN/20 (1) | F | F | F | F | F | F | A/Ai/F/G | F |
| CBN/20 (2) | F | F | F | F | F | F | G | F |
| CBN/20 (3) | F | F | F | F | F | F | F/G | F |
| CBN/19 | F | F | F | F | F | Ai/F | Ai/F/G | F |
| CBN/21 | F | F | F | F | F | F | A/Ai/F/G | F |
| CBN/22 | F | F | F | F | F | F | F/G | F |
| CBN/23 | F | F | F | F | F | F | F | F |
| MFA/20.7 | F | F | F | F | F | Ai/F | Ai/F | F |
| MFA/23.7 | F | F | F | F | F | F | F/G | F |
| MFB/23.7 | F | F | F | F | F | F | A/Ai/F/G | F |
| MFC/23.7 | F | F | F | F | F | F | A/Ai/F/G | F |
| MFD ^b | G | G | F | F | F | F | A/Ai/F/G | F/G |
| MFE ^b | F | F | F | F | F | Ai/F/G | A/Ai/F/G | F ^a |
| MFF ^b | F | F | F | F | F | Ai/F | A/Ai/G/F | F |
| Model A selected | 0/53 | 0/53 |
| Model Ai selected | 0/53 | 0/53 |
| Model F selected | 42/53 | 41/53 | 42/53 | 44/53 | 42/53 | 39/53 | 10/53 | 41/53 |
| Model G selected | 11/53 | 12/53 | 11/53 | 9/53 | 11/53 | 4/53 | 1/53 | 7/53 |
| Models F/G selected | 0/53 | 0/53 | 0/53 | 0/53 | 0/53 | 1/53 | 8/53 | 5/53 |
| Model Ai/F selected | 0/53 | 0/53 | 0/53 | 0/53 | 0/53 | 7/53 | 1/53 | 0/53 |
| Models Ai/F/G selected | 0/53 | 0/53 | 0/53 | 0/53 | 0/53 | 2/53 | 3/53 | 0/53 |
| Models A/Ai/F selected | 0/53 | 0/53 | 0/53 | 0/53 | 0/53 | 0/53 | 2/53 | 0/53 |
| All models equal | 0/53 | 0/53 | 0/53 | 0/53 | 0/53 | 0/53 | 28/53 | 0/53 |

^a The model is significantly better with a confidence level of 0.05, but not with a confidence level of 0.01.^b Samples measured by pNMR.

Table 4
Values for the mean sum of squared residuals (MSR) for the Gompertz and Foubert models

| Sample | MSR Gompertz | MSR Foubert |
|----------------|--------------|--------------|
| CBA/20 (1) | 0.345 | 0.117 |
| CBA/20 (2) | 0.250 | 0.115 |
| CBA/20 (3) | 0.244 | 0.076 |
| CBB/20 (1) | 0.092 | 0.038 |
| CBB/20 (2) | 0.073 | 0.035 |
| CBB/20 (3) | 0.213 | 0.003 |
| CBC/20 (1) | 1.630 | 0.003 |
| CBC/20 (2) | 0.895 | 0.085 |
| CBC/20 (3) | 0.621 | 0.041 |
| CBD/20 (1) | 0.345 | 0.097 |
| CBD/20 (2) | 0.138 | 0.021 |
| CBD/20 (3) | 0.046 | 0.318 |
| CBE/20 (1) | 0.044 | 0.079 |
| CBE/20 (2) | 0.063 | 0.037 |
| CBE/20 (3) | 0.017 | 0.093 |
| CBF/20 (1) | 0.562 | 0.055 |
| CBF/20 (2) | 0.010 | 0.057 |
| CBF/20 (3) | 0.478 | 0.059 |
| CBG/20 (1) | 0.128 | 0.180 |
| CBG/20 (2) | 0.328 | 0.116 |
| CBG/20 (3) | 0.431 | 0.215 |
| CBH/20 (1) | 0.138 | 0.127 |
| CBH/20 (2) | 0.017 | 0.120 |
| CBH/20 (3) | 0.045 | 0.095 |
| CBI/20 (1) | 0.409 | 0.061 |
| CBI/20 (2) | 0.638 | 0.012 |
| CBI/20 (3) | 0.282 | 0.039 |
| CBJ/20 (1) | 0.107 | 0.127 |
| CBJ/20 (2) | 0.213 | 0.096 |
| CBJ/20 (3) | 0.087 | 0.072 |
| CBK/20 (1) | 0.228 | 0.075 |
| CBK/20 (2) | 0.109 | 0.032 |
| CBK/20 (3) | 0.117 | 0.031 |
| CBL/20 (1) | 0.075 | 0.084 |
| CBL/20 (2) | 0.034 | 0.100 |
| CBL/20 (3) | 0.085 | 0.040 |
| CBM/20 (1) | 0.193 | 0.070 |
| CBM/20 (2) | 0.605 | 0.098 |
| CBM/20 (3) | 0.194 | 0.014 |
| CBN/20 (1) | 0.637 | 0.085 |
| CBN/20 (2) | 0.576 | 0.142 |
| CBN/20 (3) | 0.286 | 0.007 |
| CBN/19 | 1.831 | 0.010 |
| CBN/21 | 0.092 | 0.025 |
| CBN/22 | 0.095 | 0.007 |
| CBN/23 | 0.280 | 0.053 |
| MFA/20.7 | 0.084 | 0.029 |
| MFA/23.7 | 0.010 | 0.001 |
| MFB/23.7 | 0.150 | 0.073 |
| MFC/23.7 | 0.036 | 0.012 |
| MFD | 0.047 | 0.042 |
| MFE | 0.036 | 0.018 |
| MFF | 0.464 | 0.065 |
| Mean | 0.286 | 0.071 |
| Minimum | 0.010 | 0.001 |
| Maximum | 1.831 | 0.318 |

proposed model. For sample CB D/20(3) the fit of the Avrami model with induction time is worse than that of the Gompertz and the proposed model. When comparing the Gompertz and proposed models one can see that for sample CB N/19 (Fig. 3A/C) the Gompertz model still deviates quite a lot from the measured data points, while the proposed model hardly shows any deviation from the data points. For sample CB D/20(3) (Fig. 3B/D) both models fit the data points very well, the Gompertz model being a little better in the beginning of the crystallization process.

2.4. Evaluation of the models

The newly developed model is capable of describing the isothermal crystallization kinetics of fats much better than the generally used Avrami model. Several authors (Metin & Hartel, 1998; Toro-Vazquez et al., 2000; Wright, Hartel et al., 2000; Ziegleder, 1990) using the Avrami model have described the fit as very good, stating a correlation coefficient always greater than 0.96 (Wright, Hartel et al., 2000), an R -value between 0.993 and 0.998 (Metin & Hartel, 1998) and a regression coefficient greater than 0.998 (Toro-Vazquez et al., 2000). In this study, a mean value for R^2 of 0.9998 was obtained for the proposed model and, moreover, Fig. 3 shows that the fit for the Avrami model is far from being perfect when compared to the fit for the proposed model. It has to be remarked that Metin and Hartel (1998) and Toro-Vazquez et al. (2000) linearize the Avrami model to estimate its parameters (which is statistically questionable) while in our study non-linear regression was used to fit the data.

The Avrami model with induction time fits the data significantly better than the standard Avrami model for most of the samples (details not shown). However, the fit of the proposed model is still much better.

The Gompertz model used by Kloek et al. (2000) already offers a large improvement when compared to the Avrami model. This can be seen in Fig. 3 and also when comparing the values for the information and PRESS criteria (data not shown). When comparing the Gompertz model with the Avrami model with induction time, the Gompertz model nearly always performs better even though it uses one parameter less. The proposed model, however, performs even better than the Gompertz model in the majority of the cases. Also, it offers the advantage that it describes the crystallization kinetics of all samples used (different fats, different temperatures, different measuring methods) nearly as good, while the Gompertz model performs excellent on certain samples but significantly poorer on others.

Another advantage of the proposed model is the fact that it has been written in the form of a differential equation, which makes it easier to give a mechanistic interpretation [compare Eq. (13) to Eqs. (1)–(3) and

(18)] and to use the model when, for example, non-isothermal conditions are used. Moreover, an analytical solution is available for the isothermal situation, facilitating non-linear parameter estimation in a multitude of software packages.

A possible concern is that the Avrami model was originally developed for volume fractions of crystallization (Avrami, 1940). Replacing these volume fractions (as obtained by dilatometry) by mass fractions (as obtained in pNMR) or transition heats (as obtained in DSC) may introduce some error when the crystallization process involves more than one polymorphic form because the densities and latent heats are not the same for the different polymorphic forms. This is the case for the cocoa butter samples and one milk fat sample used in this study. The error introduced when using mass fractions will be smaller than when using transition heats since the difference in density between different polymorphic forms is smaller than the difference in latent heats. It was decided to compare the proposed model with the Avrami model for all the datasets, since in literature too DSC thermograms related to the crystallization of different polymorphic forms are fitted to the Avrami model (Kerti, 1998; Metin & Hartel, 1998; Ziegleder, 1990). It has to be stressed however, that also for datasets obtained by pNMR and for datasets obtained by DSC where only one polymorphic form is involved the proposed model performs significantly better than the Avrami model.

To get more insight in the differences between the models, their ability to fit an asymmetric curve was tested. The asymmetry of a curve was defined as:

$$\text{asym} = \frac{t_{90\%} - t_{50\%}}{t_{50\%} - t_{10\%}} \quad (20)$$

where $t_{x\%}$ is the time needed to reach $x\%$ crystallization. A symmetric curve has a value of 1 for this asym parameter.

The appendix provides the formulas obtained for asym for the different models. Here only the conclusions will be discussed.

For the Avrami model (with and without induction time) the asymmetry is only dependent on the Avrami exponent n . The values of n of the standard Avrami model obtained for the crystallization experiments described in this study coincide with asym values around 1 or smaller, meaning that the start of the crystallization is slower than the end, which is not in concordance with the experimental data, explaining why the Avrami model does not provide very good fits. The Avrami model with induction time takes care of the slow start of the crystallization process (the induction period). This leads to values of n coinciding with asym values larger than 1, which is in concordance with the experimental data, thus explaining why the Avrami model with induction time fits the data significantly better than the standard Avrami model. For the

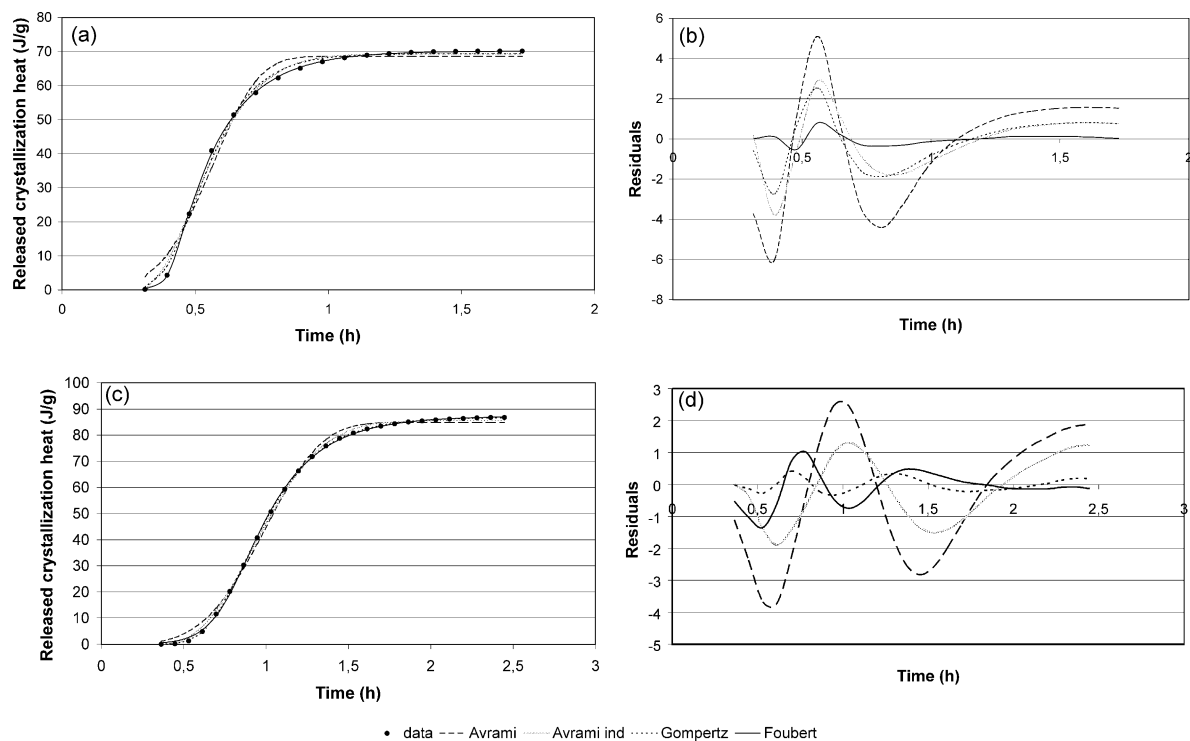


Fig. 3. Visual representation of the quality of fit of the different models. (a) and (b) represent the measured data points and the predicted curves for the three models. (c) and (d) represent the residuals as a function of time for the three models. (a) and (c) represent CBN/19, (b) and (d) CBD/20(3).

Gompertz model it turns out that the asym value is a fixed value of 1.57. This is an important feature of the model because it means that the Gompertz model does not offer any flexibility concerning the asymmetry of the curve. This explains also why the Gompertz model fits very well for certain datasets (those who show an asym value around 1.57) and considerably worse for others.

Consequently, evaluating the asym value of a dataset would allow deciding beforehand whether the Gompertz model would fit well or not. Finally, the asym value of the proposed model is dependent on the n value, with n values equal to two giving rise to symmetric curves, as described earlier.

3. Conclusion

A new model able to describe the kinetics of isothermal crystallization was presented. The model was written in the form of a differential equation, but the analytical solution under isothermal conditions was also provided. It was shown that the proposed model always performs better than the often used Avrami model (with and without induction time) and performs better than the Gompertz model in the majority of the cases. The very good fits obtained make the model a useful tool to have a better quantitative description of the crystallization processes. Whether a true physical mechanism lays beneath this goodness of fit will have to be shown in the future.

Acknowledgements

Imogen Foubert is a research assistant of the Fund for Scientific Research—Flanders (F.W.O.—Vlaanderen). Thijs Keersebilck is acknowledged for performing a lot of the analyses and Dirk De Pauw and Ingmar Nopens for the help with WEST. Barry-Callebaut, Wieze, Belgium, ADM Cocoa, Koog aan de Zaan, Netherlands, Bendsorp, Barry Callebaut, Bussum, Netherlands and Aveve Dairy Products, Klerken, Belgium are acknowledged for providing the samples. Ron Brown (SPPS Inc.) is acknowledged for support. The reviewer is acknowledged for his useful comments.

Appendix

For the four models discussed in this paper the asymmetry was calculated according to Eq. (17).

For the Avrami equation with and without induction time the same *asym* value was obtained:

$$\text{asym} = \frac{\sqrt[n]{-\ln 0.1} - \sqrt[n]{-\ln 0.5}}{\sqrt[n]{-\ln 0.5} - \sqrt[n]{-\ln 0.9}}$$

This leads to an asym value of one for values of the Avrami exponent of 3.25. Tailing is obtained for n bigger than 3.25.

For the Gompertz equation the following was obtained:

$$\text{asym} = \frac{-\ln(-\ln(0.9)) + \ln(-\ln(0.5))}{-\ln(-\ln(0.5)) + \ln(-\ln(0.1))} = 1.57$$

For the proposed model the dependence of the asym value on the model parameters is given by the following equation:

$$\text{asym} = \frac{\ln(0.5^{1-n} - 1) - \ln(0.1^{1-n} - 1)}{\ln(0.9^{1-n} - 1) - \ln(0.5^{1-n} - 1)}$$

An asym value of one is obtained for n equal to 2 and tailing is observed for n values larger than 2.

References

- Avrami, M. (1940). Kinetics of phase change. II. Transformation-time relations for random distribution of nuclei. *Journal Chemical Physics*, 8, 212–224.
- Boistelle, R. (1988). Fundamentals of nucleation and crystal growth. In N. Garti, & K. Sato (Eds.), *Crystallization and polymorphism of fats and fatty acids* (pp. 189–276). New York: Marcel Dekker.
- Foubert, I., Vanrolleghem, P. A., & Dewettinck, K. Differential scanning calorimetry method to determine the isothermal crystallization kinetics of cocoa butter. *Thermochimica acta* (accepted for publication)
- Hartel, R. W. (1992). Solid-liquid equilibrium: crystallization in foods. In H. G. Schwartzberg, & R. W. Hartel (Eds.), *Physical chemistry of foods* (pp. 47–81). New York: Marcel Dekker Inc.
- Hatakeyama, T., & Quinn, F. X. (1997). *Thermal analysis, fundamentals and applications to polymer science*. Chichester: John Wiley & Sons.
- Herrera, M. L., de Leon Gatti, M., & Hartel, R. W. (1999). A kinetic analysis of crystallization of a milk fat model system. *Food Research International*, 32(4), 289–298.
- Kawamura, K. (1979). The DSC thermal analysis of crystallization behavior in palm oil. *Journal American Oil Chemists' Society*, 56(8), 753–758.
- Kerti, K. (1998). Thermal analysis of cocoa butter and cocoa butter alternatives crystallisation using DSC method. In *2nd International Workshop on Control Applications in Post-harvest and Processing Technology* (pp.173–176). Budapest, Hungary, 3–5 June, 1998.
- Kloek, W., Walstra, P., & van Vliet, T. (2000). Crystallization kinetics of fully hydrogenated palm oil in sunflower oil mixtures. *Journal American Oil Chemists' Society*, 77(4), 389–398.
- Metin, S., & Hartel, R. W. (1998). Thermal analysis of isothermal crystallization kinetics in blends of cocoa butter with milk fat or milk fat fractions. *Journal American Oil Chemists' Society*, 75(11), 1617–1624.
- Nawar, W. (1996). Lipids. In R. Fennema Owen (Ed.), *Food chemistry* (3rd ed.) (pp. 225–319). New York: Marcel Dekker.
- Nelder, J. A., & Mead, R. (1965). A simplex method for function minimization. *Computer Journal*, 7, 308–313.

- Sharples, A. (1966). Overall kinetics of crystallization. In A. Sharples (Ed.), *Introduction to polymer crystallization* (pp. 44–59). London: Edward Arnold Ltd.
- Toro-Vazquez, J. F., Briceno-Montelongo, M., Dibildox-Alvarado, E., Charo-Alonso, M., & Reyes-Hernandez, J. (2000). Crystallization kinetics of palm stearin in blends with sesame seed oil. *Journal American Oil Chemists' Society*, 77(3), 297–310.
- Vanrolleghem, P. A., & Dochain, D. (1998). Bioprocess model identification. In J. Van Impe, P. A. Vanrolleghem, & D. Iserentant (Eds.), *Advanced instrumentation, data interpretation and control of biotechnological processes* (pp. 251–318). Dordrecht: Kluwer Academic Publishers.
- Wright, A. J., Narine, S. S., & Marangoni, A. G. (2000). Comparison of experimental techniques used in lipid crystallization studies. *Journal American Oil Chemists' Society*, 77(12), 1239–1242.
- Wright, A. J., Hartel, R. W., Narine, S. S., & Marangoni, A. G. (2000). The effect of minor components on milk fat crystallization. *Journal American Oil Chemists' Society*, 77(5), 463–475.
- Wunderlich, B. (1990). *Thermal analysis*. New York: Academic Press.
- Ziegler, G. (1990). DSC-thermal analysis and kinetics of cocoa butter crystallization. *Fat Science Technology*, 92(12), 481–485.
- Zwietering, M. H., Jongenburger, I., Rombouts, F. M., & Van't Riet, K. (1990). Modeling of the bacterial growth curve. *Applied Environmental Microbiology*, 56(6), 1875–1881.